ORIGINAL ARTICLE

Biogas and Volatile Fatty Acid Production During Anaerobic Digestion of Straw, Cellulose, and Hemicellulose with Analysis of Microbial Communities and Functions

Jie Liu[1] · Xiaoyu Zuo[1] ⬤ · Ke Peng[1] · Rui He[1] · Luyao Yang[1] · Rufei Liu[2]

Abstract

The anaerobic digestion efficiency and methane production of straw was limited by its complex composition and structure. In this study, rice straw (RS), cellulose, and hemicellulose were used as raw materials to study biogas production performance and changes in the volatile fatty acids (VFAs). Further, microbial communities and genetic functions were analyzed separately for each material. The biogas production potential of RS, cellulose, and hemicellulose was different, with cumulative biogas production of 283.75, 412.50, and 620.64 mL/(g·VS), respectively. The methane content of the biogas produced from cellulose and hemicellulose was approximately 10% higher than that produced from RS after the methane content stabilized. The accumulation of VFAs occurred in the early stage of anaerobic digestion in all materials, and the cumulative amount of VFAs in both cellulose and hemicellulose was relatively higher than that in RS, and the accumulation time was 12 and 14 days longer, respectively. When anaerobic digestion progressed to a stable stage, *Clostridium* was the dominant bacterial genus in all three anaerobic digestion systems, and the abundance of *Ruminofilibacter* was higher during anaerobic digestion of RS. Genetically, anaerobic digestion of all raw materials proceeded mainly via aceticlastic methanogenesis, with similar functional components. The different performance of anaerobic digestion of RS, cellulose, and hemicellulose mainly comes from the difference of composition of raw materials. Increasing the accessibility of cellulose and hemicellulose in RS feedstock by pretreatment is an effective way to improve the efficiency of anaerobic digestion. Since the similar microbial community structure will be acclimated during anaerobic digestion, there is no need to adjust the initial inoculum when the accessibility of cellulose and hemicellulose changes.

Keywords Process parameters · Metagenomics · Metabolic pathways · Methane metabolism

✉ Xiaoyu Zuo
   zuoxy@mail.buct.edu.cn

1   Department of Environmental Science and Engineering, College of Chemical Engineering, Beijing University of Chemical Technology, 15 BeiSanhuan East Road, ChaoYang District, Beijing 100029, People's Republic of China

2   China Urban Construction Design & Research Institute, No.36, Deshengmenwai Street, Beijing, China

Abbreviations

AD   Anaerobic digestion
RS   Rice straw
TS   Total solids
VS   Volatile solids
TC   Total carbon
TN   Total nitrogen
VFAs   Volatile fatty acids
TCD   Thermal conductivity detector
FID   Flame ionization detector
STAMP   Statistical Analysis of Metagenomic Profiles
KEGG   Kyoto Encyclopedia of Genes and Genomes
OTUs   Operational taxonomic units

Introduction

Straw is a lignocellulose agricultural waste that is produced in large quantities [1], which has both pollution and resource properties. In one hand, it may cause severe environmental pollution and threaten human health and ecosystems if utilized improperly [2]. On the other hand, straw is an excellent source of biomass with significant utilization and development potential. Utilizing straw as energy is an effective way to not only potentially solve the problem of environmental pollution caused by straw but also to ease the world energy crisis. As anaerobic digestion (AD) can degrade the organic components in biomass under mild conditions and produce a large amount of biogas, with methane as the main component, AD is considered to be one of the most suitable and promising biomass energy utilization technologies [3].

The main components of lignocellulose materials, such as straw, are cellulose, hemicellulose, and lignin, with a small amount of gum, fructose, protein, and ash [4]. Typically, the contents of cellulose, hemicellulose, and lignin are 40–50%, 25–30%, and 15–20%[5], respectively. Cellulose, hemicellulose, and lignin have different chemical structures and physicochemical properties [6]. Cellulose is a linear compound composed of D-glucopyranose units connected by β-1,4 glycosidic bonds, and there are crystalline and amorphous regions inside the cellulose molecule. It is stable in nature, and hydrogen bonding significantly reduces the accessibility and reactivity of cellulose to degradable cellulase and anaerobic microorganisms [7]. The other reason that cellulose is resistant to microorganisms is the complex components of crystalline build-up, which serve as an antidegradation barrier. Hemicellulose is composed of a variety of sugar aldehyde carboxyl groups, sugar groups, and acetyl groups [8] and is a general term for complex glycans with branched chains in their molecular structure. These branched structures form an amorphous polysaccharide with reduced crystallinity. Hence, hemicellulose is more readily hydrolyzed than cellulose. However, the more complex structure of hemicellulose than cellulose requires multiple enzymes for its hydrolysis. Lignin is an amorphous high-molecular-weight polymer, and its three-dimensional structure comprises C6–C3 units in a nonlinear and random manner through the action of C–H and C–C bonds [9]. It is also only degraded by microorganisms with great difficulty. Thus, biogas produced during AD of straw is derived from the degradation of cellulose and hemicellulose, rather than lignin.

Due to the differences in the physicochemical properties of cellulose, hemicellulose, and lignin, the anaerobic digestion performance and the changes in the material and microbial functions during AD are different. Li et al. [10] used cellulose, hemicellulose, and lignin as their mixtures of raw materials to study AD characteristics, and their results showed that hemicellulose is hydrolyzed more easily and acidified more quickly than cellulose. From the perspective of the physicochemical properties of straw raw materials, the efficiency of AD of straw was affected by the degree of exposure to microorganisms of cellulose, hemicellulose. In order to improve the efficiency of AD, extensive studies have been dedicated to destabilizing lignin, cellulose, and hemicellulose to increase microbial accessibility to cellulose and hemicellulose [11]. Based on a variety of pretreatment methods [12, 13], studies on parameters of AD [14, 15] and carbon migration of AD [16] were carried out to further improve the efficiency of AD. Furthermore, some scholars have conducted in-depth studies on microbial communities in the AD system [17, 18] and metagenomic characteristics during AD [16] of straw hoping to present a thorough understanding of the AD of straw and to provide a theoretical reference for further research into improving the performance of AD of straw. Meng et al. [19] reported the microbial community structures were similar between feedstock-to-inoculum ratios of 3 and 0.5 during solid-state thermophilic anaerobic co-digestion of pig urine and rice straw according to the metagenomic analysis results. Zhang et al. [20] found the AD of food waste was inhibited under high load suffered VFAs and aceticlastic methanogenesis was blocked, and CO_2 reduction pathway was enhanced under certain conditions. Xing et al. [21] performed a metagenomic study on methanogenic activities and pathways of different carbon source, and the results showed that the dominant methanogenic pathway was related to the carbon source. Although many studies on these topics have produced many fruitful results, there are still many unsolved problems. Does the different accessibility of cellulose and hemicellulose affect the microbial community structure and ultimately affect the efficiency of AD? Is the different efficiency of AD of materials before and after pretreatment due to the raw materials or the microbial community structure? There are very few studies in this area, and the available information is also very limited. Therefore, further studies on material changes and microbial community structure of AD with different microbial accessibility of cellulose, hemicellulose are warranted.

Studies on AD of the primary components of straw will help us to reveal the mechanisms underlying AD of straw under extreme pretreatment condition, at which accessibility of cellulose and hemicellulose becomes 100%, and the regularities of their AD will provide a basis for studying the regularities of the AD of straw.

In this study, rice straw (RS), cellulose, and hemicellulose were used as raw materials for AD. The form of carbon in the gas phase and volatile fatty acids (VFAs) in the liquid phase were investigated under identical digestion conditions. Moreover, the composition of microorganisms was determined, and genetic function analyses were performed to provide some reference for further clarifying the principle of the AD of RS.

Materials and Methods

Feedstock and Inoculum

Experimental RS was obtained from Jixian County, Tianjin. After being naturally air-dried, the whole straw was cut into small pieces of 3–4 cm using a trowel, and these

pieces were pulverized with a YSW-180 type grinder and passed through a 20-mm mesh sieve. The materials were then placed in a dry and ventilated area, ready for use. Cellulose and hemicellulose were both purchased from Beijing Jianqiang Weiye Technology Co., Ltd. They were derived from RS and had a purity of 99% and 97%, respectively. The digestion sludge of pig manure, which was taken from Shunyi District, Beijing, was used as the inoculum in the experiment. The physicochemical properties of raw materials and inoculum are provided in Table 1.

Experimental Equipment and Methods

Sealed glass bottles with a volume of 5 L were used as batch reactors. The bottle caps had two vents: one was connected to a gas-collecting device by latex and glass tubes, and the other vent was connected to a latex tube and sealed with a water stopper as an outlet. Raw materials and inoculum were added to the reactors. The substrate to inoculum ratio (S/I) was set to 2.5. The organic load, which was based on total solids (TS), of raw materials was 50 g/L, and the organic load of inoculum was 20 g/L. Pure water was added to the organic load to adjust the effective volume of the AD reactor to 4 L, and the initial pH in the reaction device was adjusted to 6.8–7.2 by adding $Ca(OH)_2$. The carbon nitrogen (C/N) ratio was adjusted to 25:1. The AD reaction device was placed in a 35 °C ± 1 °C constant-temperature water bath to enable mesophilic AD. The AD time was set to 40 days, and the quantity of biogas produced, and its composition was measured every day. The anaerobic digestion experiment of inoculum as the raw material had been performed, and the data were subtracted as background values. In addition, the VFA concentration of the sludge in the reaction system was measured daily. Each group of experiments was designed with three parallel experiments, and the data are the average of these three parallel experiments.

Table 1 The physicochemical characteristics of raw material and inoculum

Indexes	Rice straw	Cellulose	Hemicellulose	Inoculum
Total solid (TS)[a] (%)	93.70	98.86	96.02	11.59
Volatile solid (VS)[a] (%)	80.82	96.46	96.02	7.61
Total carbon (TC)[b] (%)	38.14	44.44	42.75	35.15
Total nitrogen (TN)[b] (%)	0.51	0.00	0.00	2.50
C/N	74.78	–	–	14.06
Cellulose[b] (%)	40.43	99.00	0.00	ND
Hemicellulose[b] (%)	29.27	0.00	97.00	ND
Lignin[b] (%)	5.17	0.00	0.00	ND
Ammonia nitrogen (mg/L)	–	–	–	853

[a]Content of fresh matter

[b]Content of dry matter

Analytical Methods

Analysis of Biogas Production Performance

The water displacement method was used to record daily biogas production [22]. A SP-2100 gas chromatograph (BeiFenRuiLi, Beijing, China), which was furnished with a TDX-01molecular sieve and a thermal conductivity detector (TCD), was used to determine the CH_4, CO_2, H_2, and N_2 composition of the biogas, and argon was used as the carrier gas. The temperatures of the oven, injector port, and TCD were 140 °C, 150 °C, and 150 °C, respectively.

Chemical Composition Analysis

Total solids (TSs) and volatile solids (VSs) were measured using APHA standard methods [23]. The total carbon (TC) and total nitrogen (TN) were determined using a Vario EL/micro cube elemental analyzer (Elementar, Germany). The composition of cellulose, hemicelluloses, and lignin in the RS and digestate was measured using an A2000I fiber analyzer (ANKOM, USA). Samples were taken from the sampling port of the anaerobic digester every day to measure VFAs. A GC-2014 gas chromatograph (Shimadzu, Japan) was used to analyze the VFAs, and a flame ionization detector (FID) was equipped in the gas chromatograph. The gas chromatograph column was a capillary column of 30 m × 0.25 mm × 0.25 μm (Agilent, DB-WAX), and the carrier gas that was used was nitrogen. The operational temperatures of the injector, detector, and column were 250 °C, 250 °C, and 180 °C, respectively.

Kinetic Analysis

The modified Gompertz model was used in this study to evaluate AD performance. It is the most widely used model for the analysis of AD processes of complex organic matter [24].

The modified Gompertz model formula is shown in Eq. (1):

$$P_{(t)} = P_m \times exp\left\{ -exp\left[\frac{R_m}{P_m}(\lambda - t) + 1\right] \right\} \tag{1}$$

where $P_{(t)}$ is the degree of hydrolysis/gasification of the material on day t (%), P_m is the maximum degree of hydrolysis/gasification (%), R_m represents the maximum hydrolysis/gasification rate (%), λ is the delay time (d), t is the digestion time (d), and e is the natural constant, 2.71828.

Microbial Community and Metagenome Analysis

DNA Extraction

DNA extraction was performed using an EZNA Soil DNA Kit (Omega Bio-tek, Nor-cross, GA, US), DNA concentration and purity were detected using NanoDrop2000, and the quality of DNA extraction was detected using 1% agarose gel electrophoresis.

Microbial Community Analysis

Two primers were used for polymerase chain reaction (PCR) amplification of the V3-V4 variable region: 338F (5′-ACTCCTACGGGAGGCAGCAG-3′) and 806R (5′-GGACTA CHVGGGTWTCTAAT-3′).

Purified amplified fragments were constructed into pair-end library using the Illumina MiSeq platform (Illumina, San Diego, CA, USA) and following standard operating procedures. Sequencing was then performed using the Illumina MiSeq PE300 platform (Shanghai majorbio Biomedical Technology Co., Ltd.).

The raw sequences were determined using Trimmomatic software for quality control and FLASH software for splicing. UPARSE software (version 7.1 http://drive5.com/uparse/) was then used, and the sequences were clustered based on 97% similarity of operational taxonomic units (OTUs). Single sequences and chimeras were removed. The ribosomal database processor classifier (http://rdp.cme.msu.edu/) was used to annotate the species classification of each sequence, and these were compared with data in the Silva database (SSU132), using an alignment threshold of 70%.

Metagene Analysis

The DNA was fragmented using Covaris M220 (Gene Corporation, China), and a fragment of about 400 bp was interrupted by screening. A PE library was constructed using a NEXTFLEX Rapid DNA-Seq (BioScientific, USA) library construction kit. A PE library Metabonomic sequencing was then performed sequenced after bridge PCR amplification using the Illumina NovaSeq/Hiseq Xten (Illumina, USA) sequencing platform.

Fastp software was used to perform quality control on the raw data, and BWA software was used to align the reads to the host's DNA sequence and remove contaminated reads with high similarity. The stitching software MEGAHIT, which is based on the principle of succinct de Bruijn graphs, was used to stitch and assemble optimized sequences. Contigs $\geq$ 300 bp were selected as the final assembly result in the splicing results. MetaGene was used to perform open reading frame (ORF) prediction on the assembled contig, and then CD-HIT software was used to cluster the predicted gene sequences of all samples to construct a non-redundant gene set. Finally, using SOAPaligner software, the high-quality reads of each sample were compared with non-redundant gene sets (95% identity), and the gene abundance information in the corresponding samples was counted.

BLASTP was used to align non-redundant gene set sequences with the Kyoto encyclopedia of genes and genomes (KEGG) gene database (GENES). KEGG orthology-based annotation system (KOBAS) 2.0 was used for function annotation based on the results of

the comparison. The sum of gene abundances corresponding to KO, Pathway, EC, and Module was used to calculate the abundance of corresponding functional categories.

Data Analysis

Statistics and data processing were performed using Microsoft Excel software. Origin 9.0 software was used for dot-line, histogram, and nonlinear fitting. The composition of microbial communities and their genetic functions were analyzed using the ggplot2 package of R language for Windows 3.5. 1. Fisher's exact test was performed using the Statistical Analysis of Metagenomic Profiles (STAMP).

Results and Discussion

Biogas Production Performance

The AD performances of RS, cellulose, and hemicellulose are shown in Fig. 1. The daily biogas production of RS and its main components contained two daily gas production peaks during the entire AD process (Fig. 1A). The intensity of the first peak was lower than that of the second peak for RS digestion. In contrast, the first gas production peaks from cellulose and hemicellulose digestion were higher than the second. Among
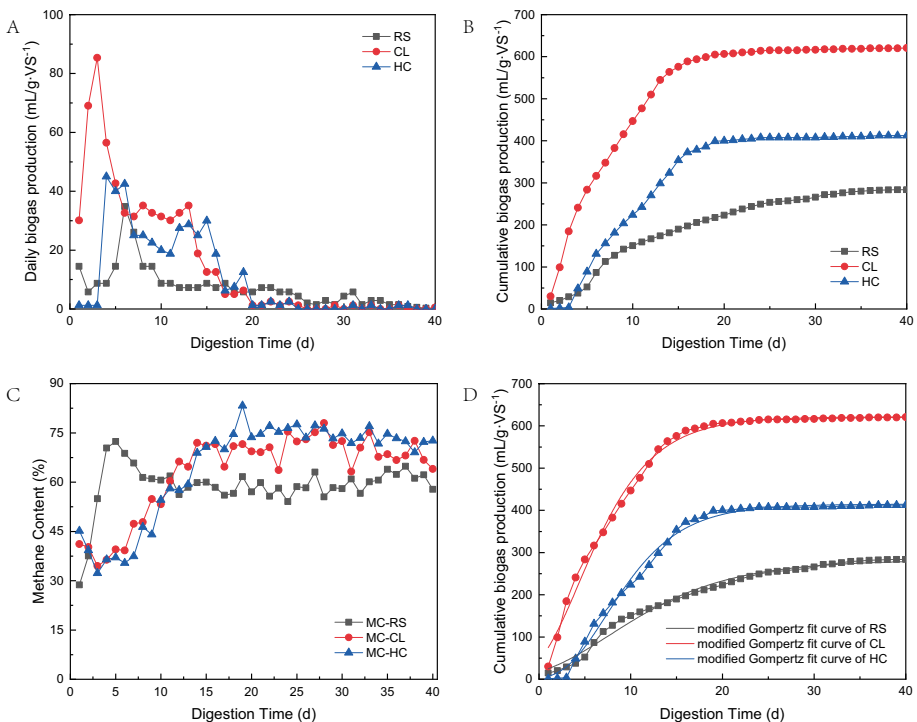

Fig. 1 The daily biogas production (**A**), cumulative biogas production (**B**), methane content (**C**), and modified Gompertz fit curve of the cumulative biogas production (**D**) of RS, CL and HC

them, production peaks of RS digestion occurred on the first and sixth days, and biogas production on these days was 14.19 and 34.78 mL/(g·VS), respectively. The two biogas production peaks of cellulose appeared on the third and twelfth days, and biogas production on these days was 85.36 and 35.64 mL/(g·VS), respectively. The first biogas production peak of cellulose was 501.55% higher than that of RS. The second biogas production peak of cellulose was similar to the second gas production peak of RS. The two biogas production peaks of hemicellulose appeared on the fourth and fourteenth days, with production on these days of 45.00 and 30.00 mL/(g·VS), respectively. The first biogas production peak was 217.12% higher than that of RS digestion, and the second biogas production peak was 15.71% lower. The peaks of biogas production of RS occurred significantly earlier than those of cellulose and hemicellulose. This may be because RS contains fructose and other substances, in addition to cellulose and hemicellulose, which are more anaerobically digestible [4], leading to the early start of the AD process.

For cumulative biogas production, cellulose had the highest at 620.64 mL/(g·VS), followed by hemicellulose at 412.50 mL/(g·VS), and RS at 283.75 mL/(g·VS) (Fig. 1B). The cumulative gas production of cellulose and hemicellulose was 118.72% and 45.37% higher than that of RS, respectively. These results are consistent with those of Li et al. [1, 10]. This is because the VS of RS is lower than that of cellulose and hemicellulose, which also contain lignin. Studies have shown that lignin is composed of three main monomers: coumaryl alcohol, coniferyl alcohol, and sinapyl alcohol. These basic monomers constitute the basic structural unit of lignocellulose: syringyl phenylpropane (S), guaiacyl phenylpropane (G), and p-hydroxyphenylpropane (H) [25]. Lignin is challenging to biodegrade under anaerobic conditions [26, 27]. Indeed, in straw, cellulose, hemicellulose, and lignin form structures that are difficult to biodegrade [9, 11]. In addition, some cellulose and hemicellulose cannot be used by microorganisms in RS, so its cumulative gas production is significantly lower than that of cellulose and hemicellulose. Inhibition mechanisms may also contribute to the difficulty of biodegrading enzymes to adsorb to hydrophobic lignin [28].

For the methane content during AD, RS first showed a slow increase, reaching a maximum of 72.39% on the fifth day, and then gradually decreased to 61.44% on the eighth day, finally stabilizing at around 60% (Fig. 1C). The trends for cellulose and hemicellulose were similar: both exhibited a slow increase in the early stage of AD and stabilized at approximately 70% after day 14. Before day 12, the methane content of RS was higher than that of cellulose and hemicellulose. After 12 days, the methane contents of cellulose and hemicellulose were higher than that of RS, which might have occurred because RS is harder to hydrolyze than cellulose and hemicellulose [29]. In the early stage of AD, when there were insufficient methanogens to consume large amounts of acetic acid, more small molecule acids (SMAs) were generated in the system, and methanogenesis was inhibited to a certain extent. As methanogens grow, the SMAs were gradually consumed, and methanogenesis became more active and more efficient at producing methane. The amount of accumulated SMA was low in the early stage of AD of RS, and methanogenesis was also less inhibited. Therefore, the methane content of RS was higher than that of cellulose and hemicellulose in the early stage of AD. However, the low number of accumulated SMA also resulted in fewer methane-producing substrates, which result in less efficiency at producing methane than cellulose and hemicellulose in the later stage of AD. This is consistent with the results of microbial community structure analysis. After the methane content stabilized, the methane content of the biogas produced from cellulose and hemicellulose was approximately 10% higher than that produced from RS. The research results of Li [10] and Wang [29] also showed that AD of cellulose and hemicellulose produced more methane than that of straw.

Table 2 The parameters estimated by the modified Gompertz model

Substrate	Parameter			
	P_m/g	R_m/g	λ/day	R^2
Rice straw	282.03	37.67	0.15	0.98711
Cellulose	621.42	138.17	− 0.12	0.99311
Hemicellulose	414.60	91.95	2.86	0.99384

The pH level, ammonia nitrogen content, and total alkalinity are important indices that can be used to evaluate the stability of anaerobic digestive systems and microbial metabolism. The pH levels of the digestion sludge of RS, cellulose and hemicellulose were 7.33, 7.29, and 7.25, respectively, and the alkalinity levels were 4500, 4200, and 4100 mg/L, respectively. The values for each of these parameters were within the normal range: pH > 6.8 and alkalinity > 2000 mg/L [30]. In addition, the ammonia nitrogen contents of RS, cellulose, and hemicellulose were 710, 720, and 735 mg/L, respectively, which did not exceed the tolerance range of anaerobic microorganisms, which is 2 g/L. The methane production process was not suppressed [31], and the system reached a stable status after AD.

The modified Gompertz model was used to fit the dynamics of AD of RS, cellulose, and hemicellulose to the dynamics of biogas production. The correlation coefficient, R^2, of the experimental value and the fitted value were above 0.98 (Fig. 1D; Table 2). The maximum biogas production of the fitted value was very similar to the cumulative biogas production.
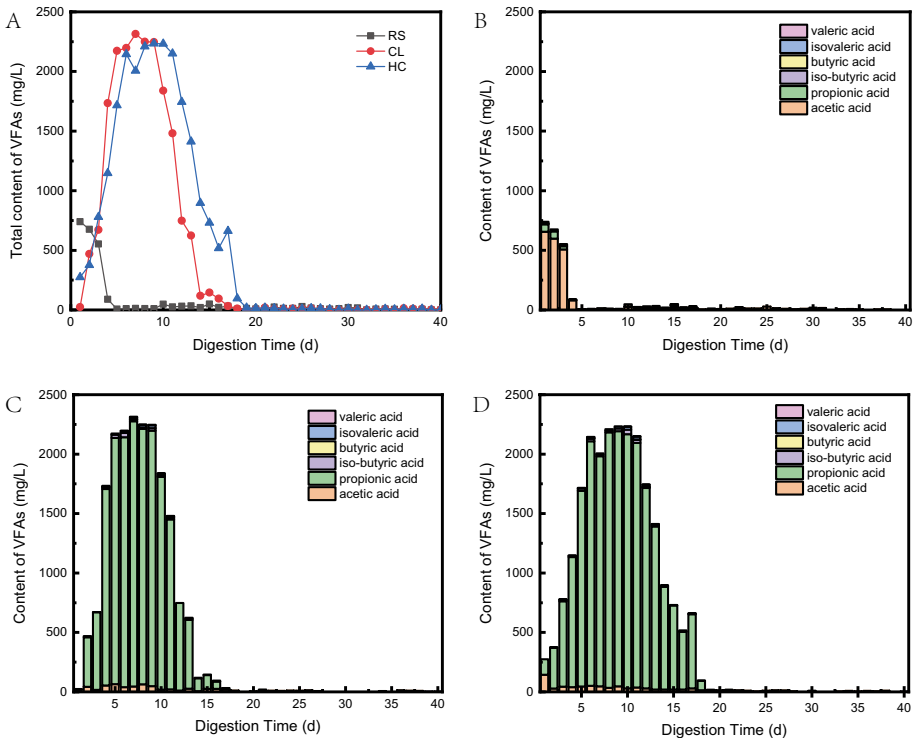
Fig. 2 The changes of total concentration of VFAs (**A**), and content of VFAs of RS (**B**), CL (**C**) and HC (**D**) during the anaerobic digestion

The biogas production rates R_m of cellulose and hemicellulose were 266.79% and 144.09% higher than the R_m of RS, respectively, and hemicellulose showed the longest lag time.

Volatile Fatty Acids

VFAs are important intermediate metabolites in the process of AD and are one of the indicators that characterize the performance of AD [32]. Changes in VFAs during AD of RS, cellulose, and hemicellulose are shown in Fig. 2. The accumulation of VFAs occurred in the early stages of AD of all three raw materials (Fig. 2A). As AD proceeded, the accumulated VFAs were consumed. The accumulation stages of VFAs during AD of RS, cellulose, and hemicellulose were 4, 16, and 18 days, respectively. The concentration of VFAs from RS digestion was highest on day 1 (740.12 mg/L), while VFA concentration from cellulose reached its maximum on day 7 at 2414.29 mg/L and was 3.26 times the highest concentration of RS. The maximum concentration of VFAs from hemicellulose was reached on day 9, which was 2234.58 mg/L and was 3.01 times the highest concentration of RS. The VFA concentration of RS stabilized below 50 mg/L from day 5, and cellulose and hemicellulose stabilized below 50 mg/L from days 16 and 18, respectively. According to Lee et al. [33], VFA concentration above 6000 mg/L suppresses AD. As VFA concentration in this study did not exceed 2500 mg/L, expectations were met in that no suppressive effects were seen. It has been reported that xylan in lignocellulose promotes the swelling of cellulose, thereby increasing its enzymatic hydrolysis [34], which may be the reason why RS enters a hydrolytic acidification condition earlier than cellulose and hemicellulose.

Studies have shown that acetic acid is the main carbon source for the AD of methane production, and other VFAs, including propionic acid, are also mostly converted into acetic acid to be inserted into methane metabolism by microorganisms [35]. The composition of VFAs is closely related to the performance of AD [36]. For the composition of VFAs produced during AD of the three raw materials (Fig. 2B, C , D), the main component of the cumulative stage from day 1 to day 4 of RS was acetic acid (88.38–91.88%). For cellulose, the acetic acid content was highest on day 1 (79.08%), and the main component for days 2–16 was propionic at 65.70–98.42%. Similar results were observed for hemicellulose for days 1–18. Acetic acid (52.60%) dominated the first day, and propionic acid was the main component for days 2–18 at 81.57–97.19%. Studies have shown that VFAs with even- and odd-numbered carbon are beneficial for the synthesis of 3-hydroxybutyrate and 3-hydroxyvalerate [37], respectively, while 3-hydroxybutyrate is more beneficial for the methanation process. The accumulation of substantial amounts of propionic acid could inhibit the AD process [37]. Studies by Pullammanappallil et al. [38] showed that the maximum accumulation of propionic acid was 2750 mg/L, which did not inhibit AD. In this study, the maximum cumulative concentrations of propionic acid of cellulose and hemicellulose were 2149.01 and 2148.60 mg/L, respectively, neither of which exceeded 2750 mg/L. Inhibition of digestion is thus not likely. When the AD progressed into the stable biogas production stage, and the methane content remained stable, the accumulated propionic acid was quickly consumed.

In this study, the concentration of VFAs produced from the AD of RS reached a maximum value before cellulose and hemicellulose, but its maximum concentration was lower than that of the other two components. This finding was consistent with the regularities of biogas production that was discussed before. Similar to VFAs, the biogas yield of RS was lower than that of cellulose and hemicellulose. The main component of VFAs that accumulated during the AD of RS was acetic acid, which was quickly consumed. The major

component of VFAs that accumulated during the AD of cellulose and hemicellulose was propionic acid, which accumulated over an extended period. This finding is consistent with the regularities of methane content during the AD of these three materials, and it shows that the production of VFAs had a dual effect on the efficiency and biogas production performance of AD. On the one hand, VFAs are substrates for methanogenesis. Within a certain concentration range, the accumulation of VFAs is positively correlated with biogas production. On the other hand, the excessive accumulation of VFAs will also lead to the inhibition of AD.

Microbial Community

After splicing all the sequences, quality control, and filtering out the low-quality sequences, a total of 175,423 bacterial sequences and 132,506 archaeal sequences were obtained. A total of 534 bacterial OTUs and 21 archaeal OTUs were obtained. These 534 bacterial OTUs belong to 31 different phyla, 60 different classes, 94 different orders, 142 different families, and 243 different genera. The 21 archaeal OTUs obtained belonged to four different phyla, six different classes, seven different orders, 11 different families, and 15 different genera.
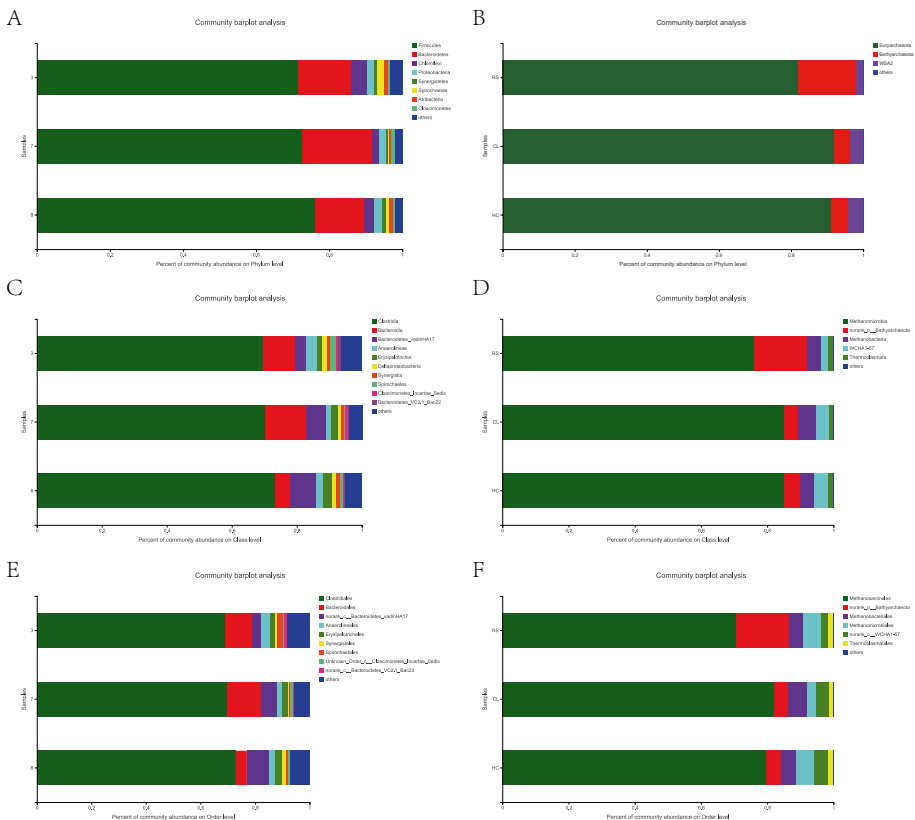

Fig. 3 Microbial community of bacteria (**A**) and archaea (**B**) at phylum level, microbial community of bacteria (**C**) and archaea (**D**) at class level, microbial community of bacteria (**E**) and archaea (**F**) at order level

The composition of microbial communities at the phylum, class, and order level is shown in Fig. 3. At the phylum level, the dominant community of bacteria was *Firmicutes*, followed by *Bacteroidetes*, and the dominant community of archaea was *Euryarchaeota*, followed by *Bathyarchaeota*. The results were similar as the results gained by Liu et al. [39]. *Firmicutes* and *Bacteroidetes* are two typical bacteria phyla, which can degrade cellulose and use organic acids as final metabolites [33, 40]. *Euryarchaeota* was an archaeal phylum that uses methane as final metabolic product [41]. *Bathyarchaeota* was an archaeal phylum with acetyl-CoA-centralized metabolism [42], which can degrade protein [43]. The abundance of *Euryarchaeota* in the stable stage of AD of cellulose and hemicellulose was higher than that in the AD of RS. The result explained the higher methane content in the AD of cellulose and hemicellulose than in the AD of RS. The abundance of *Bathyarchaeota* in the stable stage of AD of RS was higher than that in the stable stage of AD of cellulose and hemicellulose. This result was consistent with the complex chemical composition of RS. At the class and order level, the
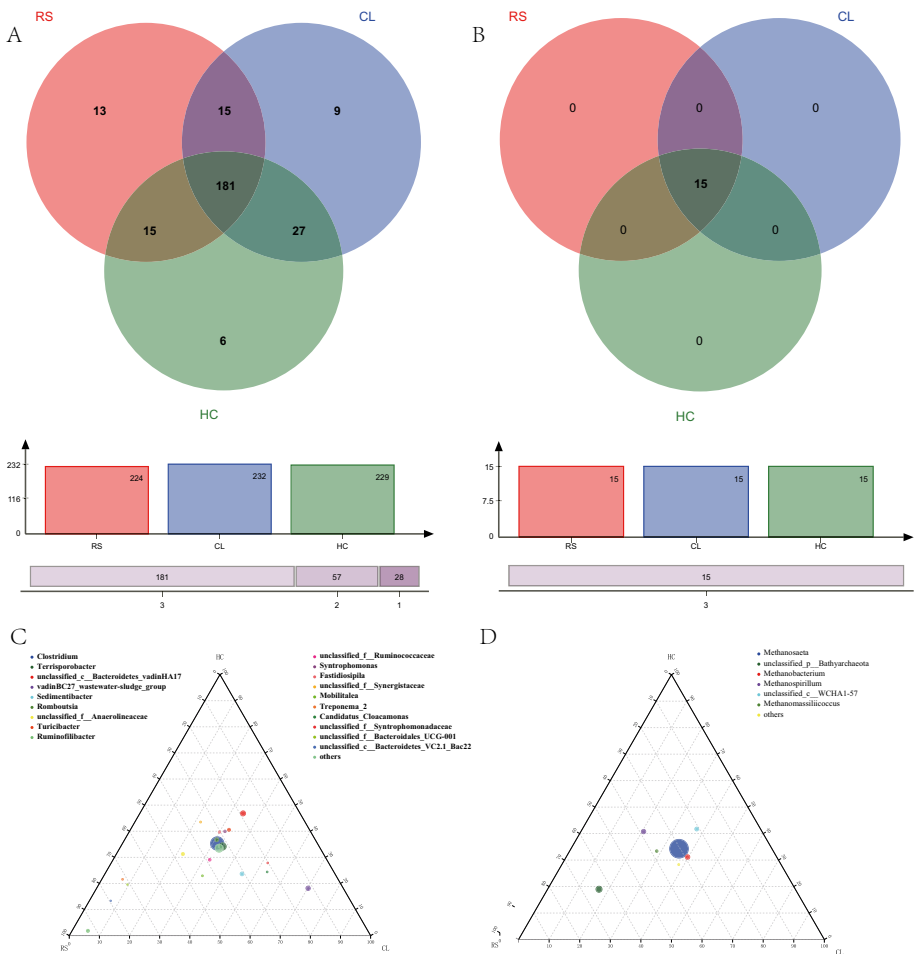

Fig. 4 Venn analyze of bacterial (**A**) and archaea (**B**), and community structures of bacterial (**C**) and archaea (**D**) at genus level

dominant communities of bacteria were *Clostridia* and *Clostridiales*, and the dominant communities of archaea were *Methanomicrobia* and *Methanosarcinales*, respectively.

The composition of microbial communities at the genus level is shown in Fig. 4. In the bacterial Venn diagram (Fig. 4A), the data show that most of the bacteria in the three raw materials were the same, with 181 genera accounting for 74.49% of the total bacterial genera. The number of bacterial genera unique to the AD systems of RS, cellulose, and hemicellulose was 13, 9, and 6, respectively. In the archaeal Venn diagram (Fig. 4B), the data show that the archaeal genus in the AD systems of the three raw materials was the same.

As shown in the ternary phase diagram of the bacteria (Fig. 4C), *Clostridium* was the dominant genus in the AD systems of RS, cellulose, and hemicellulose, with relative abundances of 38.44%, 43.14%, and 40.62%, respectively. The second most abundant genus was *Terrisporobacter* with relative abundances of 12.29%, 12.42%, and 11.65% for the AD systems of RS, cellulose, and hemicellulose, respectively. In addition, the abundances of *Sedimentibacter* and *Romboutsia* in the AD systems of the three raw materials were also very similar. *Ruminofilibacter* showed a higher abundance in RS AD and a lower abundance in cellulose and hemicellulose ADs. *Bacteroidetes* vadinHA17 and vadinBC27 wastewater sludge groups were present in the cellulose and hemicellulose AD systems in higher abundances than in the RS system. The abundance of *Bacteroidetes* vadinHA17 in the cellulose AD system was higher than in the hemicellulose AD system, and the abundance of the vadinBC27 wastewater sludge group in the hemicellulose AD system was significantly higher than in the cellulose AD system.

In the process of anaerobic acidification, carbohydrates are hydrolyzed into ethanol, lactic acid, acetic acid, and butyric acid by monosaccharide fermentation acid-producing bacteria, and lactic acid is further reduced to propionic acid. At the same time, VFAs are mutually converted by redox reactions under the action of different microorganisms. *Clostridium* plays an important role in degrading organic components and generating VFAs [44]. For example, Merlino et al. [45] found that *Clostridium* can degrade wood fibers and vegetarian raw materials. *Terrisporobacter* is a strictly anaerobic bacterium that can degrade carbohydrate raw materials into acetic acid [46]. In this study, the abundances of *Clostridium* and *Terrisporobacter* were relatively high, which provided a suitable environment for the smooth progress of the hydrolysis and acidification process in the AD system. It has been reported that the vadinBC27 wastewater sludge group produced small molecular fatty acids from fermentable amino acids, cysteine, leucine, methionine, serine, tryptophan, and valine [47] and was well adapted to ammonia nitrogen concentrations [48].

We found that the substrates available for methane production in our study were very limited. This is consistent with *Methanosaeta*, which can only use acetic acid as a substrate for AD [49] to produce CH_4. On the other hand, *Methanobacterium* produces methane through CO_2 reduction with hydrogen [50], and *Methanomassiliicoccus* produces methane by reducing methanol [51]. From the ternary phase diagram of the archaea (Fig. 4D), it is evident that *Methanosaeta* is the dominant bacterium in the AD systems of the three raw materials, with similar abundances of 81.66%, 79.24%, and 70.22% for the AD systems of RS, cellulose, and hemicellulose, respectively. *Methanobacterium* abundances were 5.39%, 4.23%, and 3.96%, and *Methanomassiliicoccus* abundances were 1.30%, 1.52%, and 1.74% for the AD systems of RS, cellulose, and hemicellulose, respectively, indicating that the AD of the three raw materials was based primarily on the reduction of acetic acid.

Functional Analysis

A total of 35.66 GB of data was obtained via high-throughput sequencing. Based on the original sequencing data, the low-quality and N-reads in the data were eliminated, and 331,859,324 high-quality sequences, required for subsequent analysis, were obtained. A total of 4,533,413 gene sequences were predicted using ORF prediction. Then, our results were compared with the KEGG database to obtain the functional annotations of each sample. The functional composition of the three raw materials at levels 1, 2, and 3 were found to be similar. At level 1, metabolism was the most abundant pathway with relative abundances of 68.46%, 68.62%, and 68.56% of the AD systems of RS, cellulose, and hemicellulose, respectively. At level 2, carbohydrate metabolism was the most abundant pathway, with relative abundances of 15.42%, 15.35%, and 15.29% of the AD systems of RS, cellulose, and hemicellulose, respectively. At level 3, the most abundant metabolic pathway was biosynthesis of amino acids with relative abundances of 5.22%, 5.15%, and 5.15% of the AD systems of RS, cellulose, and hemicellulose, respectively, followed by carbon metabolism, with relative abundances of 5.04%, 5.11%, and 5.03 of the AD systems of RS, cellulose, and hemicellulose, respectively. The relative abundances of methane metabolism were 2.26%, 2.41%, and 2.29% of the AD systems of RS, cellulose, and hemicellulose, respectively. This is consistent with the findings of Li et al. [52] and the chemical composition of the raw materials.

At the module level, a total of four modules were related to methane production: M00357, M00567, M00356, and M00563. Of these, M00357 uses acetate as a substrate, M00567 uses $H_2\text{-}CO_2$, M00356 uses methanol, and M00563 is based on methylamine-dimethylamine-trimethylamine. The abundances of these four modules are shown in Table 3. M00357 accounted for the highest proportion of modules, with relative abundances of 47.10%, 47.62%, and 47.15% for the AD systems of RS, cellulose, and hemicellulose, respectively, followed by M00567 with relative abundances of 28.40%, 28.65%, and 28.98% for the AD systems of RS, cellulose, and hemicellulose, respectively (Table 3). The next was M00356, whose relative abundances were 23.07%, 22.51%, and 22.65% for the AD systems of RS, cellulose, and hemicellulose, respectively, and M00563 had the lowest relative abundances, which were 1.43%, 1.22%, and 1.21% for the AD systems of RS, cellulose, and hemicellulose, respectively. The results were similar with the findings of Chen [16]. These results indicate that the methanogenic process in this study was aceticlastic methanogenesis, which is also consistent with the analysis results of microbial communities.

The functional composition at the enzyme level is shown in Fig. 5A, which was compared with methane metabolism metabolic pathway map00680. The results in Fig. 4 show that the most abundant pathway in this study is that acetic acid first produces acetyl-CoA, then undergoes a series of reactions to produce 5-methyl-5,6,7,8-tetrahydromethane, then biosynthesizes methyl-CoM, and finally produces methane. The dominant pathway is

Table 3 The abundance of modules related to methane generation on module level

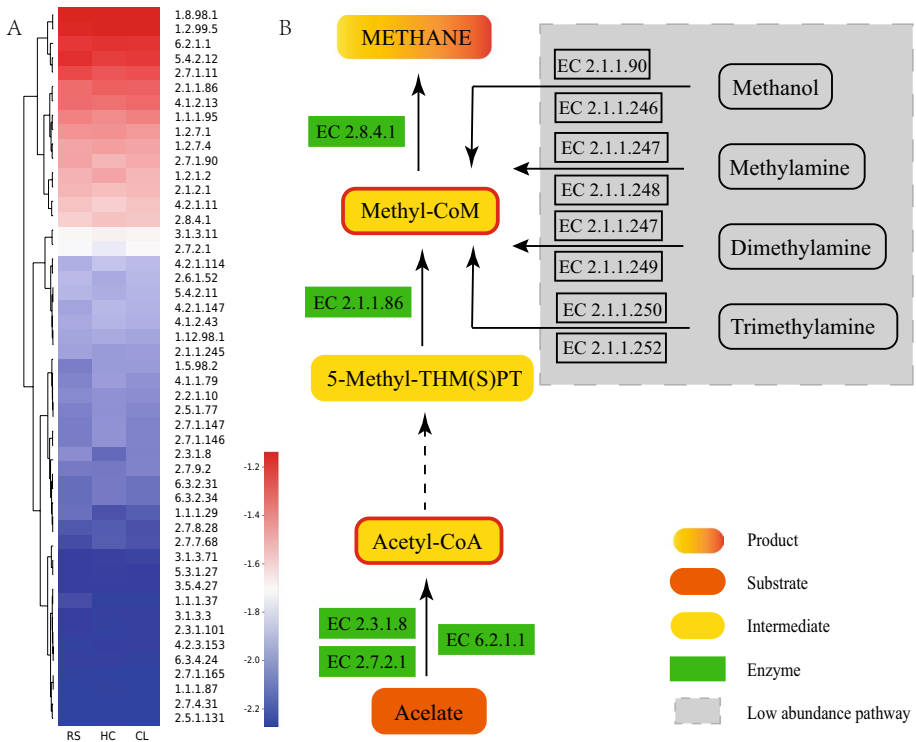| Module	RS	CL	HC	Total
M00357	172,436	161,772	180,200	514,408
M00567	103,960	97,314	110,754	312,028
M00356	84,442	76,450	86,572	247,464
M00563	5238	4148	4628	14,014

Fig. 5 Composition of functions (**A**) at enzyme level and the abundance pathway (**B**)

shown in Fig. 5B. Unlike the results reported by Pore [53], aceticlastic methanogenesis was more abundant than hydrogenotrophic methanogenesis in this study. According to Conrad [54], more than 67% of methane was produced via aceticlastic methanogenesis. This difference might be due to the initial microbial composition in the inoculum; the heterotrophic or chemolithotrophic acetogenesis is enhanced in the inoculum in this study.

The methyl coenzymes methyl-CoM and acetyl-CoA [55] were important enzymes in the methanogenesis pathway. There are five pathways that can produce methyl-CoM [56]. In this study, 5-methyl-THM (S) PT produced the highest abundance of methyl-CoM through the action of enzyme EC 2.1.1.86, with relative abundances of 83.19%, 86.22%, and 86.14% for the AD systems of RS, cellulose, and hemicellulose, respectively. This result is consistent with the findings of Du [55].

It can be seen from the regularities of VFA production that acetic acid, propionic acid, and butyric acid were important intermediate products in the process of AD in this study. At enzyme level, there were 30, 6, and 5 enzymes related to acetic acid, propionic acid, and butyric acid, respectively. The enzyme abundance of total enzymes related to acetic acid, propionic acid, and butyric acid is shown in Fig. 6. The result showed that the abundance of enzymes related to acetic acid metabolism was the highest, followed by propionic acid and then butyric acid, which was similar with the result reported by Chen [16]. According to the results of VFAs discussed previously, in the stable stage of AD in this study, the accumulated acetic acid, propionic acid, and butyric acid were consumed, and the methanogenesis was stabilized. Besides methanogenesis via aceticlastic methanogenesis in this
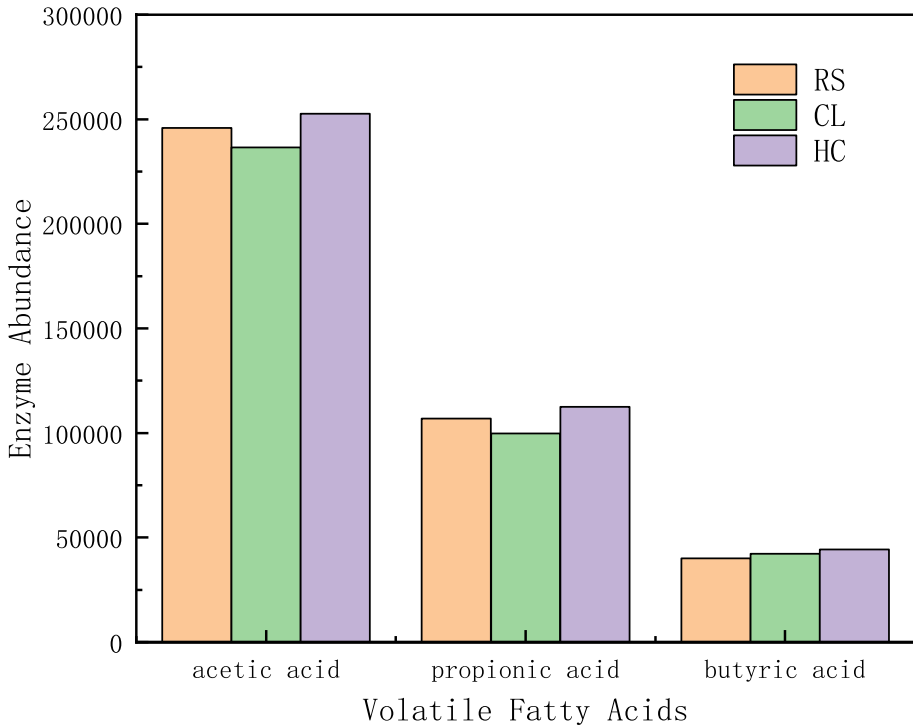
Fig. 6 Enzyme abundance associated with the formation or degradation of acetic acid, propionic acid, and butyric acid

study as we discussed, the high abundance of enzymes related to the acetic acid metabolism was reasonable. The abundance of enzymes related to metabolism of acetic acid, propionic acid, and butyric acid was similar in the AD systems of all the three raw materials. This result is consistent with the results of microbial community structure.

Fisher's exact test analysis in the STAMP difference analysis was used to compare the abundance of functions between two samples. Through this analysis, significant difference functions could be obtained. The gene set was constructed and annotated with methane metabolism and acetyl-CoA-related genes, and the abundance was calculated using the RPKM method. At the module level, the function of microorganisms in the AD systems of RS, cellulose, and hemicellulose was analyzed using STEMP. As shown in Fig. 7, there is a significant difference between RS and cellulose in the acetyl-CoA-related genes (Fig. 7A). The results indicate that there are two deviations exceeding 1: the highest deviation is M00036, followed by M00088, with the deviations $+3.55$ and -3.30, respectively. The difference between RS and hemicellulose in the acetyl-CoA-related genes (Fig. 7B) was the same as that for cellulose. The two modules with the highest deviations were $+3.33$ and -2.76, respectively. The function of M00036 is to convert leucine to acetoacetate and acetyl-CoA, and the function of M00088 is to convert acetyl-CoA to acetoacetate, 3-hydroxybutyrate, or acetone. In the significant difference analysis of RS and cellulose in methane metabolism (Fig. 7C), it was evident that the highest deviation was M00001, which is $+0.50$. Its function is to convert glucose to pyruvate from straw
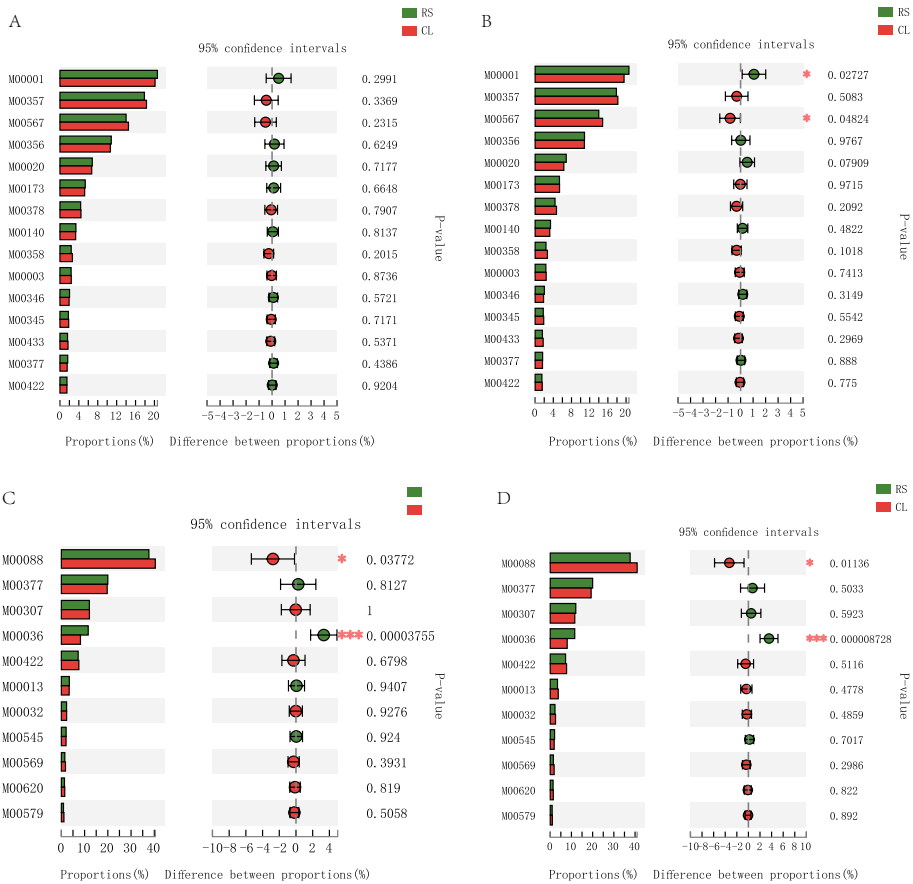
Fig. 7 Fisher's exact test of RS and CL (**A**), RS and HC (**B**) on acetyl-CoA-related genes, and Fisher's exact test of TS and CL (**C**), RS and HC (**D**) on methane metabolism related genes

to hemicellulose. The significant difference analysis of RS and hemicellulose in methane metabolism (Fig. 7D) showed that one of the absolute values of deviation was greater than 1 — M00001, the same as cellulose, with a deviation of + 1.07. The results show that the AD process of RS, cellulose, and hemicellulose had little difference in the function of microorganisms during the methanogenesis stage, while the functions of microorganisms related to acetyl-CoA were quite different.

Conclusions

The material changes of the AD of RS, cellulose, and hemicellulose showed marked differences. The biogas production potential of cellulose and hemicellulose was greater than that of RS. In the early stages, VFAs accumulated in all the three AD systems and the cumulative amount of cellulose and hemicellulose were higher than that of RS, and the period of accumulation of cellulose and hemicellulose was longer than that of RS. When the AD progressed to the stable stage, *Clostridium* was the dominant bacterial genus in

all three AD systems. The AD of all three raw materials proceeded mainly via aceticlastic methanogenesis, with similar components of gene. The difference of AD performance of RS, cellulose, and hemicellulose mainly stems from the difference in the composition of raw materials. Increasing the accessibility of cellulose and hemicellulose in RS feedstock by pretreatment is an effective way to improve the AD efficiency. When the accessibility of cellulose and hemicellulose changes, there is no need to adjust the inoculum, as the similar microbial community structure will be acclimated.

Author Contribution Xiaoyu Zuo initiated the project and was responsible for coordinating the entire study and its funding. Ke Peng and Rui He completed most of the experiments. Jie Liu assisted in completing the experiment and analyzing the experimental data and wrote the manuscript. Luyao Yang and Rufei Liu modified the grammar of the article appropriately.

Data Availability All data of biogas and VFAs generated or analyzed during this study are included in this manuscript. The raw reads of 16 s RNA were deposited into the NCBI Sequence Read Archive (SRA) database (Accession Number: SRR12131890). The raw reads of metagenome were deposited into the NCBI Sequence Read Archive (SRA) database (Accession Number: SRPSRR12132972).

Declarations

Competing Interests The authors declare no competing interests.

References

1. Li, K., Liu, R., Cui, S., Yu, Q., & Ma, R. (2018). Anaerobic co-digestion of animal manures with corn stover or apple pulp for enhanced biogas production. *Renewable Energy, 118*, 335–342.
2. Li, J., Wachemo, A. C., Yu, G., & Li, X. (2019). Enhanced anaerobic digestion performance of corn stalk pretreated with freezing-thawing and ammonia: An experimental and theoretical study. *Journal of Cleaner Production, 247*, 119112.
3. Liu, Y., Wachemo, A. C., Yuan, H., & Li, X. (2019). Anaerobic digestion performance and microbial community structure of corn stover in three-stage continuously stirred tank reactors. *Bioresource Technology, 287*, 121339.
4. McKendry, P. (2002). Energy production from biomass (part 1) overview of biomass. *Bioresource Technology, 83*, 37–46.
5. Houfani, A. A., Anders, N., Spiess, A. C., Baldrian, P., & Benallaoua, S. (2020). Insights from enzymatic degradation of cellulose and hemicellulose to fermentable sugars-a review. *Biomass and Bioenergy, 134*, 10581.
6. Behera, S., Arora, R., Nandhagopal, N., & Kumar, S. (2014). Importance of chemical pretreatment for bioconversion of lignocellulosic biomass. *Renewable and Sustainable Energy Reviews, 36*, 91–106.
7. Jeffrey, G. A., & Saenger, W. (1994). *Hydrogen binding in biological structure second printing*. Springer.
8. Xiao, B., Sun, X. F., & Sun, R. (2001). Chemical, structural, and thermal characterizations of alkali-soluble lignins and hemicelluloses, and cellulose from maize stems, rye straw, and rice straw. *Polymer Degradation and Stability, 74*, 307–319.
9. Gao, L., Chen, S., & Zhang, D. (2017). Advances in modifying lignin structures for largely enhancing high-lignin biomass saccharification. *Process Biochemistry, 57*, 175–180.
10. Li, W., Khalid, H., Zhu, Z., Zhang, R., Liu, G., Chen, C., & Thorin, E. (2018). Methane production through anaerobic digestion: Participation and digestion characteristics of cellulose, hemicellulose and lignin. *Applied Energy, 226*, 1219–1228.

11. Lai, C., Tu, M., Xia, C., Shi, Z., Sun, S., Yong, Q., & Yu, S. (2017). Lignin alkylation enhances enzymatic hydrolysis of lignocellulosic biomass. *Energy & Fuels, 31*(11), 12317–12326.

12. Hjorth, M., Gränitz, K., Adamsen, A. P. S., & Møller, H. B. (2011). Extrusion as a pretreatment to increase biogas production. *Bioresource Technology, 102*(8), 4989–4994.

13. Liu, C. M., Wachemo, A. C., Yuan, H. R., Zou, D. X., Liu, Y. P., Zhang, L., Pang, Y. Z., & Li, X. J. (2018). Evaluation of methane yield using acidogenic effluent of NaOH pretreated corn stover in anaerobic digestion. *Renewable Energy, 116*, 224–233.

14. Li, L., Peng, X., Wang, X., & Wu, D. (2018). Anaerobic digestion of food waste: A review focusing on process stability. *Bioresource Technology, 248*(Pt A), 20–28.

15. Boe, K., Batstone, D. J., Steyer, J.-P., & Angelidaki, I. (2010). State indicators for monitoring the anaerobic digestion process. *Water Research, 44*(20), 5973–5980.

16. Chen, D., Zuo, X., Li, J., Wang, X., & Liu, J. (2020). Carbon migration and metagenomic characteristics during anaerobic digestion of rice straw. *Biotechnology for Biofuels, 13*, 130.

17. Cai, Y., Hua, B., Gao, L., Hu, Y., Yuan, X., Cui, Z., Zhu, W., & Wang, X. (2017). Effects of adding trace elements on rice straw anaerobic mono-digestion: Focus on changes in microbial communities using high-throughput sequencing. *Bioresource Technology, 239*, 454–463.

18. Azman, S., Khadem, A. F., Lier, J. B. V., Zeeman, G., & Plugge, C. M. (2015). Presence and role of anaerobic hydrolytic microbes in conversion of lignocellulosic biomass for biogas production. *Critical Reviews in Environmental Science and Technology, 45*(23), 2523–2564.

19. Meng, L., Xie, L., Kinh, C. T., Suenaga, T., Hori, T., Riya, S., Terada, A., & Hosomi, M. (2018). Influence of feedstock-to-inoculum ratio on performance and microbial community succession during solid-state thermophilic anaerobic co-digestion of pig urine and rice straw. *Bioresource Technology, 252*, 127–133.

20. Zhang, W., Li, L., Wang, X., Xing, W., Li, R., Yang, T., & Lv, D. (2020). Role of trace elements in anaerobic digestion of food waste: Process stability, recovery from volatile fatty acid inhibition and microbial community dynamics. *Bioresource Technology, 315*, 123796.

21. Xing, L., Yang, S., Yin, Q., Xie, S., Strong, P. J., & Wu, G. (2017). Effects of carbon source on methanogenic activities and pathways incorporating metagenomic analysis of microbial community. *Bioresource Technology, 244*(Pt 1), 982–988.

22. Guan, R., Li, X., Wachemo, A. C., Yuan, H., Zuo, X., & Gu, J. (2018). Enhancing anaerobic digestion performance and degradation of lignocellulosic components of rice straw by combined biological and chemical pretreatment. *Science of the Total Environment, 637–638*, 9–17.

23. Zuo, X., Yuan, H., Wachemo, A. C., Wang, X., Zhang, L., Li, J., Wen, H., Wang, J., & Li, X. (2019). The relationships among sCOD, VFAs, microbial community, and biogas production during anaerobic digestion of rice straw pretreated with ammonia. *Chinese Journal of Chemical Engineering, 28*(1), 286–292.

24. Nopharatana, A., Pullammanappallil, P. C., & Clarke, W. P. (2007). Kinetics and dynamic modelling of batch anaerobic digestion of municipal solid waste in a stirred reactor. *Waste Management, 27*(5), 595–603.

25. Frommhagen, M., Sforza, S., Westphal, A. H., Visser, J., Hinz, S. W. A., Koetsier, M. J., van Berkel, W. J. H., Gruppen, H., & Kabel, M. A. (2015). Discovery of the combined oxidative cleavage of plant xylan and cellulose by a new fungal polysaccharide monooxygenase. *Biotechnology for Biofuels, 8*, 101.

26. Datta, R., Kelkar, A., Baraniya, D., Molaei, A., Moulick, A., Meena, R. S., & Formanek, P. (2017). Enzymatic degradation of lignin in soil: A review. *Sustainability, 9*(7), 1163.

27. Feofilova, E. P., & Mysyakina, I. S. (2016). Lignin: Chemical structure, biodegradation, and practical application (a review). *Applied Biochemistry and Microbiology, 52*(6), 573–581.

28. Zhao, C., Yan, H., Liu, Y., Huang, Y., Zhang, R., Chen, C., & Liu, G. (2016). Bio-energy conversion performance, biodegradability, and kinetic analysis of different fruit residues during discontinuous anaerobic digestion. *Waste Management, 52*, 295–301.

29. Wang, X., Cheng, S., Li, Z., Men, Y., & Wu, J. (2020). Impacts of cellulase and amylase on enzymatic hydrolysis and methane production in the anaerobic digestion of corn straw. *Sustainability, 12*(13), 5453.

30. Rajagopal, R., Massé, D. I., & Singh, G. (2013). A critical review on inhibition of anaerobic digestion process by excess ammonia. *Bioresource Technology, 143*, 632–641.

31. Lin, J., Zuo, J., Gan, L., Li, P., Liu, F., Wang, K., Chen, L., & Gan, H. (2011). Effects of mixture ratio on anaerobic co-digestion with fruit and vegetable waste and food waste of China. *Journal of Environmental Sciences, 23*(8), 1403–1408.

32. Yuan, H., Guan, R., Wachemo, A. C., Zhu, C., Zou, D., Li, Y., Liu, Y., Zuo, X., & Li, X. (2019). Enhancing methane production of excess sludge and dewatered sludge with combined low frequency CaO-ultrasonic pretreatment. *Bioresource Technology, 273*, 425–430.

33. Lee, J., Kim, J. R., Jeong, S., Cho, J., & Kim, J. Y. (2017). Long-term performance of anaerobic digestion for crop residues containing heavy metals and response of microbial communities. *Waste Management, 59*, 498–507.

34. Ju, X., Engelhard, M., & Zhang, X. (2013). An advanced understanding of the specific effects of xylan and surface lignin contents on enzymatic hydrolysis of lignocellulosic biomass. *Bioresource Technology, 132*, 137–145.

35. Chen, S., Liu, G., Zhang, R., Qin, B., & Luo, Y. (2012). Development of the microbial electrolysis desalination and chemical-production cell for desalination as well as acid and alkali productions. *Environmental Science and Technology, 46*(4), 2467–2472.

36. Lay, J.-J., Li, Y.-Y., & Noike, T. (1997). Influences of pH and moisture content on themethane production in high-solids sludge digestion. *Water Research, 31*, 1518–1524.

37. Capson-Tojo, G., Ruiz, D., Rouez, M., Crest, M., Steyer, J.-P., Bernet, N., Delgenès, J.-P., & Escudié, R. (2017). Accumulation of propionic acid during consecutive batch anaerobic digestion of commercial food waste. *Bioresource Technology, 245*(Pt A), 724–733.

38. Pullammanappallil, P. C., Chynoweth, D. P., Lyberatos, G., & Svoronos, S. A. (2001). Stable performance of anaerobic digestion in the presence of a high concentration of propionic acid. *Bioresource Technology, 78*, 165–169.

39. Liu, C., Wachemo, A. C., Tong, H., Shi, S., Zhang, L., Yuan, H., & Li, X. (2018). Biogas production and microbial community properties during anaerobic digestion of corn stover at different temperatures. *Bioresource Technology, 261*, 93–103.

40. Song, L., Song, Y., Li, D., Liu, R., & Niu, Q. (2019). The auto fluorescence characteristics, specific activity, and microbial community structure in batch tests of mono-chicken manure digestion. *Waste Management, 83*, 57–67.

41. Zou, H., Chen, Y., Shi, J., Zhao, T., Yu, Q., Yu, S., Shi, D., Chai, H., Gu, L., He, Q., & Ai, H. (2018). Mesophilic anaerobic co-digestion of residual sludge with different lignocellulosic wastes in the batch digester. *Bioresource Technology, 268*, 371–381.

42. Feng, X., Wang, Y., Zubin, R., & Wang, F. (2019). Core metabolic features and hot origin of Bathyarchaeota. *Engineering, 5*(3), 498–504.

43. Lazar, C. S., Baker, B. J., Seitz, K., Hyde, A. S., Dick, G. J., Hinrichs, K. U., & Teske, A. P. (2016). Genomic evidence for distinct carbon substrate preferences and ecological niches of Bathyarchaeota in estuarine sediments. *Environmental Microbiology, 18*(4), 1200–1211.

44. Cheng, J., Li, H., Zhang, J., Ding, L., Ye, Q., & Lin, R. (2019). Enhanced dark hydrogen fermentation of Enterobacter aerogenes/HoxEFUYH with carbon cloth. *International Journal of Hydrogen Energy, 44*(7), 3560–3568.

45. Merlino, G., Rizzi, A., Schievano, A., Tenca, A., Scaglia, B., Oberti, R., Adani, F., & Daffonchio, D. (2013). Microbial community structure and dynamics in two-stage vs single-stage thermophilic anaerobic digestion of mixed swine slurry and market bio-waste. *Water Research, 47*(6), 1983–1995.

46. Cho, H. U., Kim, Y. M., & Park, J. M. (2018). Changes in microbial communities during volatile fatty acid production from cyanobacterial biomass harvested from a cyanobacterial bloom in a river. *Chemosphere, 202*, 306–311.

47. Abe, K., Ueki, A., Ohtaki, Y., Kaku, N., Watanabe, K., & Ueki, K. (2012). Anaerocella delicata gen. nov., sp. nov., a strictly anaerobic bacterium in the phylum Bacteroidetes isolated from a methanogenic reactor of cattle farms. *Journal of General & Applied Microbiology, 58*(6), 405–412.

48. Buhlmann, C. H., Mickan, B. S., Jenkins, S. N., Tait, S., Kahandawala, T. K. A., & Bahri, P. A. (2019). Ammonia stress on a resilient mesophilic anaerobic inoculum: Methane production, microbial community, and putative metabolic pathways. *Bioresource Technology, 275*, 70–77.

49. Smith, K. S., & Ingram-Smith, C. (2007). Methanosaeta, the forgotten methanogen? *Trends in Microbiology, 15*(4), 150–155.

50. Chellapandi, P., Bharathi, M., Sangavai, C., & Prathiviraj, R. (2018). Methanobacterium formicicum as a target rumen methanogen for the development of new methane mitigation interventions: A review. *Veterinary and Animal Science, 6*, 86–94.

51. Dridi, B., Fardeau, M. L., Ollivier, B., Raoult, D., & Drancourt, M. (2012). Methanomassiliicoccus luminyensis gen. nov., sp. nov., a methanogenic archaeon isolated from human faeces. *International Journal of Systematic and Evolutionary Microbiology, 62*(Pt 8), 1902–1907.

52. Li, N., He, J., Yan, H., Chen, S., & Dai, X. (2017). Pathways in bacterial and archaeal communities dictated by ammonium stress in a high solid anaerobic digester with dewatered sludge. *Bioresource Technology, 241*, 95–102.

53. Pore, S. D., Engineer, A., Dagar, S. S., & Dhakephalkar, P. K. (2019). Meta-omics based analyses of microbiome involved in biomethanation of rice straw in a thermophilic anaerobic bioreactor under optimized conditions. *Bioresource Technology, 279*, 25–33.

54. Conrad, R. (2020). Importance of hydrogenotrophic, aceticlastic and methylotrophic methanogenesis for methane production in terrestrial, aquatic and other anoxic environments: A mini review. *Pedosphere, 30*(1), 25–39.

55. Du, M., Liu, X., Wang, D., Yang, Q., Duan, A., Chen, H., Liu, Y., Wang, Q., & Ni, B. J. (2021). Understanding the fate and impact of capsaicin in anaerobic co-digestion of food waste and waste activated sludge. *Water Research, 188*, 116539.

56. Feng, K., Wang, Q., Li, H., Du, X., & Zhang, Y. (2021). Microbial mechanism of enhancing methane production from anaerobic digestion of food waste via phase separation and pH control. *Journal of Environmental Management, 288*, 112460.